ATTITUDE CONTROL FOR MICRO SATELLITES USING ONLY MAGNETIC ACTUATION

F. Renk

Institute of Space Systems, University of Stuttgart
Pfaffenwaldring 31, 70550 Stuttgart, Germany

Abstract

Due to the constraints implied by conforming to the CubeSat standard the attitude control of such a micro satellite is a challenging task. Passive stabilization methods have been successfully used, but for certain mission requirements active attitude control is necessary. In the following an active magnetic attitude control system for the detumbling and 3-axes stabilization of CubeSats and its limitations due to in-orbit perturbations is introduced. Additionally simulation data for CASSat currently under development at the University of Sydney will be presented.

1 INTRODUCTION

The CubeSat standard introduced by the California Polytechnic State University is a widely accepted standard for micro satellites. This standard limits the size of the satellite to an edge length of 10 cm and the weight to less than 1 kg. These micro satellites are often used as educational projects at universities since they provide feasible real space projects for students. The Australian Centre for Field Robotics, University of Sydney, is currently building the CASSat. The main payload of the CASSat shall consist of a radiometer for temperature measurement of the Earth's surface. Since the radiometer shall point to a certain area on the Earth's surface and disturbance torques are acting on the satellite, an active attitude control system is required.

Developing an Attitude Determination and Control System (ADCS) for such a small satellite is challenging, not only because of the geometrical, electrical and computational power limits of a CubeSat, but also because of the CubeSat standard that prohibits pyrotechnical devices or propellant. This limits the methods that can actually be used for the attitude control.

Hence a design for the attitude control was chosen that uses only magnetic coils, so called magnetorquers, to generate control torques. The magnetic field generated by these magnetorquers interacts with the Earth's magnetic field and causes torques on the satellite. These torques are used to compensate disturbance torques and to change the attitude of the CubeSat.

This choice complicates the controller design through the fact that the system is mathematically not controllable at any given time. Torques can only be generated in the plane perpendicular to the Earth's magnetic field vector, thus in the direction of the magnetic field vector control torques can not be generated. For inclined orbits (with the exception of an inclination of 90 degrees) the system gains control over time, since the magnetic field vector changes its direction with respect to the inertial system. Hence torques can be applied on all axis over time. This fact leads to the conclusion that a system that uses only magnetic coils for actuation should be able to acquire a certain attitude whilst the disturbance torques are small.

Controllers for such a control problem have been investigated for the Ørsted satellite and were succesfully implemented. However, the Ørsted satellite can not be compared to a CubeSat since it had additional passive stabilization by a 12 m gravity gradient boom. The controller design for the Ørsted satellite has previously been adapted by CubeSat development teams from Norway and Denmark [1]. However, no data was returned form both missions so far and some of the assumptions made for the controller design seem to be unrealistic compared to other space missions and design guidelines [2].

Thus, a study on the afore mentioned control problem was performed under the particular requirement that no other control torques than the magnetic ones and no passive stabilization are applied. The controller was then implemented in a Matlab/Simulink environment to investigate its behavior in the presence of disturbance torques.

2 MAGNETIC ACTUATION

The generation of control torques using magnetorquer is limited. The following example tries to explain why

these limitation exist. A satellite equipped with magnetorquers in all three axes can generate an arbitrary magnetic dipole $\vec{m}_{satellite}$ but no matter in which direction the dipole is generated, it will always generate a torque perpendicular to the present magnetic field vector $\vec{B}_{Earth}$

$$\vec{T}_{control} = \vec{m}_{satellite} \times \vec{B}_{Earth}. \quad (1)$$

In Fig. 1 two examples for the generation of torques are given. The Earth's magnetic field vector is in the y-z-plane for this example. The plane normal to the magnetic field vector is shown. A demanded torque about the x-axis $T_{demanded-x}$ can be generated ($T_{generated-x}$), because the demanded torque vector is perpendicular to the magnetic field vector.

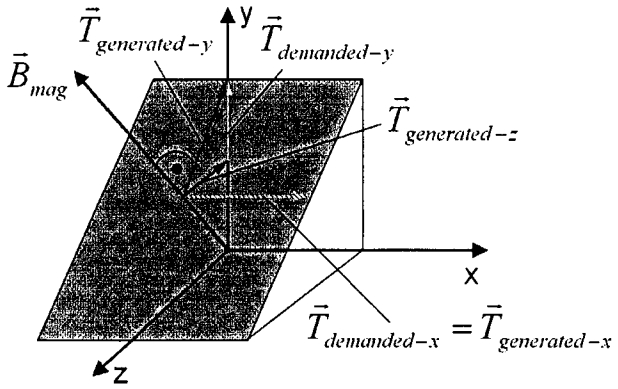

Fig. 1: *Limitations in the torque generation when using magnetorquers as actuators*

The situation looks different when a torque about the y-axis of the satellite is demanded $T_{demanded-y}$. This torque can not be generated solely, because the demanded torque is not perpendicular to the magnetic field vector. Nevertheless a torque can be generated $T_{generated-y}$, which has the desired torque component on the y-axis. But if this torque is generated, an additional torque component on the z-axis $T_{generated-z}$ will occur. This torque can be seen as internal disturbance torque on the z-axis. Depending on the angle between the desired torque and the magnetic field vector, the component of this internal disturbance torque can be higher than the desired component itself. It is obvious that generating the desired torque $T_{desired-y}$ would not make any sense.

3 EQUATIONS OF MOTION

The dynamic equations of motion relate the torques acting on the satellite to its angular velocities with respect to the inertial coordinate system. The kinematic equations relate the angular velocities of the satellite to the actual attitude [3].

3.1 Dynamic Equation

The dynamic equation with respect to a body-fixed reference frame is

$$\mathbf{I} \cdot \dot{\vec{\omega}} + \dot{\mathbf{I}} \cdot \vec{\omega} + \vec{\omega} \times (\mathbf{I} \cdot \vec{\omega}) = \vec{T}. \quad (2)$$

From Equation (2), the dynamic equation for the derivative of the angular velocities with respect to the body-fixed reference frame can be derived assuming that the inertia matrix $\mathbf{I}$ is constant.

$$\dot{\vec{\omega}} = \mathbf{I}^{-1} \cdot \left[\vec{T} - \vec{\omega} \times (\mathbf{I} \cdot \vec{\omega})\right] \quad (3a)$$

$$\vec{T} = \vec{T}_{Control} + \vec{T}_{GG} + \vec{T}_{Disturbance} \quad (3b)$$

Equation (3) can be integrated to obtain $\vec{\omega}$. The result can then be substituted into the kinematic Equation 4 that uses the quaternion attitude representation to obtain the actual attitude of the satellite. A detailed derivation of these equations can be found in [4]

$$\begin{bmatrix} \dot{q}_1 \\ \dot{q}_2 \\ \dot{q}_3 \\ \dot{q}_4 \end{bmatrix} = \frac{1}{2} \cdot \begin{bmatrix} 0 & \omega_3 & -\omega_2 & \omega_1 \\ -\omega_3 & 0 & \omega_1 & \omega_2 \\ \omega_2 & -\omega_1 & 0 & \omega_3 \\ -\omega_1 & -\omega_2 & -\omega_3 & 0 \end{bmatrix} \cdot \begin{bmatrix} q_1 \\ q_2 \\ q_3 \\ q_4 \end{bmatrix} \quad (4)$$

The Equations (3) and (4) can be linearized with respect to the required setpoint (e.g. nadir or inertial pointing of a desired axis) to enable the application of standard linear control theory. Since only the gravity gradient torque can be assumed to be dependent on the attitude for circular orbits, it can be incorporated to increase the accuracy of the controller design. The detailed derivation can be found in [5].
The linearized equations can now be combined to gain a state space model of the satellites attitude motion about the given setpoint.

$$\dot{\vec{x}} = \mathbf{A}\vec{x} + \mathbf{B} \cdot \vec{u} \quad (5)$$

with

$$\vec{x} = \begin{bmatrix} \delta\omega \\ \delta q \end{bmatrix} \quad \text{and} \quad \vec{u} = \vec{T}_{Control} + \vec{T}_{Dist} \quad (6)$$

4 DETUMBLING CONTROLLER

This controller shall control the angular momentum of the satellite after its deployment from the P-Pod or after a failure. The controller must ensure that the system reaches a state where the 3-axes attitude controller is able to stabilize the system, using only the measurement of the magnetic field to detumble the satellite and thus not relying on any other attitude determination devices and information on the orbital parameters.

Such a controller is called a B-dot controller. Since the control of the angular rates is only based on the measurement of the magnetic field vector the controller is very simple and thus provides a good reliability.
The measurement of the magnetic field using the magnetometer is used to calculate the angular velocity of the satellite. Since only changes perpendicular to the magnetic field vector can be measured only angular velocities perpendicular to the magnetic field vector can be reduced at a given time. For certain orbits the magnetic field vector changes its direction over time. Thus, the angular velocities on all axes can be reduced during the satellite's movement in its orbit.
In the following the stability of such a controller will be shown using Lyapunov stability theory.

4.1 Lyapunov Theory

The Lyapunov Theory used for showing the stability of the B-dot controller will be introduced here shortly. More detailed information on Lyapunov Stability can be found in [6] and [7].
A dynamical system can be written as the following

$$\frac{dx}{dt} = \Phi(x,t). \tag{7}$$

Since the B-dot controller will not depend on the time, an autonomous system can be considered, so Equation (7) becomes

$$\frac{dx}{dt} = \Phi(x). \tag{8}$$

Now the mathematical definition of stability due to Lyapunov is:
The equilibrium state $x = x^*$ is stable if, for any $\epsilon > 0$, there exists $\delta > 0$, such that $|x(0)| < \delta$ implies $|x(t)| < \epsilon$ for all $t > 0$. In other words, the system trajectory can be kept arbitrarily close to the origin by starting sufficiently close to it.
An equilibrium point x^* is asymptotically stable if it is stable, and in addition there exists $\delta > 0$ such that $|x(0)| < \delta$ implies that $x(t) \rightarrow x^*$ as $t \rightarrow \infty$.
Using these definitions, the following stability theorems can be derived. Let $\Theta(x)$ be a scalar function with continuous first partial derivatives in a finite neighborhood I.

$$\begin{array}{ll} T1 & \Theta(x) > 0 \forall x \neq x^* \text{ in } I, \Theta(x^*) = 0 \\ T2 & \dot{\Theta} \leq 0 \forall x \neq x^* \text{ in } I \\ T3 & \dot{\Theta} \text{ is not identically 0 for } x(t), \text{ except } x^* \\ T4 & \Theta(x) \exists \text{ in the entire state space and} \\ & \Theta(x) \rightarrow \infty, \text{ as } \|x\| \rightarrow \infty \end{array} \tag{9}$$

If T1 and T2 are fulfilled, the equilibrium state x^* is stable. If T1, T2 and T3 are fulfilled, the equilibrium state x^* is locally asymptotically stable. If T1 - T4 are fulfilled, the equilibrium state x^* is globally asymptotically stable.

4.2 Stability of B-dot Controller

Using the Lyapunov theory explained, the stability of the B-dot controller can now be shown. Choosing the rotational energy as the Lyapunov function θ and the rotation rate $\vec{\omega}$ as the state yields to the following:

$$\Theta = \frac{1}{2}\vec{\omega}^T \mathbf{I}\vec{\omega} > 0, \vec{\omega} \neq 0. \tag{10}$$

Since only the magnetic field vector is used for the rate estimation of the satellite full rate information is not available and so only the components perpendicular to the magnetic field vector can be measured. According to [8] the measured angular velocity becomes

$$\vec{\omega}_M = \left[\mathbf{E} - \vec{b}\vec{b}^T\right]\vec{\omega}. \tag{11}$$

The next step to show Lyapunov stability is to examine the derivative of the Lyapunov function. With a constant moment of inertia Equation (2) becomes

$$\mathbf{I}\dot{\vec{\omega}} + \vec{\omega} \times \mathbf{I}\vec{\omega} = \vec{T} \tag{12}$$

and using this equation in the equation for the derivative of Θ yields to

$$\begin{aligned} \dot{\Theta} &= \frac{1}{2}\left(\dot{\vec{\omega}}^T \mathbf{I}\vec{\omega} + \vec{\omega}^T \mathbf{I}\dot{\vec{\omega}}\right) = \vec{\omega}^T \mathbf{I}\dot{\vec{\omega}} = \\ &= \vec{\omega}^T\left(-\vec{\omega} \times \mathbf{I}\vec{\omega} + \vec{T}\right) = \vec{\omega}^T \vec{T}_{control} \end{aligned} \tag{13}$$

Using the control law

$$\vec{T}_{control} = -\mathbf{K} \cdot \vec{\omega}_M \tag{14}$$

with $\mathbf{K}$ being a positive definite matrix yields in the derivative

$$\dot{\Theta} = -\vec{\omega}^T \mathbf{K}\vec{\omega}_M = -\vec{\omega}^T \mathbf{K}\left[\mathbf{E} - \vec{b}\vec{b}^T\right]\vec{\omega} \leq 0. \tag{15}$$

The matrix $\mathbf{K}\left[\mathbf{E} - \vec{b}\vec{b}^T\right]$ is positive definite as long as the vector $\vec{b}$ does not become a principal axis and thus the derivative is negative definite. This fulfills the stability theorems T1-T3. Furthermore $\Theta \rightarrow \infty$ for $\omega \rightarrow \infty$ so T4 is also fulfilled and the system is globally asymptotically stable.
With $\vec{b}$ being a principle axis, the matrix is only positive semi-definite and the system can only be assumed to be stable, but not asymptotically stable.

Using magnetic torquers for the actuation of the satellite always has the limitation that torques can only be applied perpendicular to the magnetic field. However in this case this is not a limitation because only torques perpendicular to the magnetic field are required. The angular velocities parallel to the magnetic field vectors can not be measured and hence a control of these velocities is irrelevant at a given time.

$$\vec{T}_{control} = -\mathbf{K} \cdot \vec{\omega}_M = \vec{m}_{control} \times \vec{B} \tag{16}$$

$$\vec{m}_{control} = \mathbf{K}_{control} \vec{\omega}_M \times \vec{B} \tag{17}$$

Since the cross product $\vec{\omega}_M \times \vec{B}$ points in the direction of $\dot{\vec{B}}$ the control law can be simplified to the B-dot-controller

$$\vec{m}_{control} = \mathbf{K}_{control} \dot{\vec{B}} \tag{18}$$

In the above stability consideration the magnetic field vector was seen as constant in the inertial system. This is not exactly accurate, but since the change in the magnetic field vector is very small compared to the angular velocities measured this change was neglected in these considerations.
Nevertheless the change in the magnetic field is important for the cases when the measured axis is a principal axis of rotation. Because of the change in the magnetic field vector the magnetic field vector will become a non principal axis and the satellite will still be able to detumble in all three axis.

5 3-AXES CONTROLLER

Three controllers were examined for the control problem of the Ørsted satellite [9]:

1. Finite Horizon Controller
2. Infinite Horizon Controller
3. Constant Gain Controller

The finite horizon controller provides the best performance, however, this controller has a very high computational burden, since the Riccati Equation has to be solved on board.
For the infinite horizon controller the Riccati Equation can be solved off-line, but the memory demand to store the time variant feedback matrix is rather high. This makes the implementation of these two controllers extremely difficult on a CubeSat.
Since the accuracy of the constant gain controller does not significantly decrease it was chosen for implementation. The constant gain controller has the major disadvantage that the feedback matrix has to be calculated for one particular orbit and is not suitable for any other orbit. If the planned orbit is not reached or the orbit is changed the feedback matrix has to be recalculated and uploaded into the controller.

5.1 The 3-Axes Control Problem

In the linearized Equation (5) the input vector $\vec{u}$ consists of torques. Since CASSat shall only be actuated by magnetorquers, the control torques $\vec{T}_{Control}$ can not be generated directly. The magnetorquer can generate a magnetic dipole moment $\vec{m}_{ctrl}$ that results in a control torque because of the interaction with the Earth's magnetic field. The generated torque can be calculated with

$${}^b\vec{T}_{ctrl}(t) = {}^b\vec{m}_{ctrl}(t) \times {}^b\vec{B}(t) \tag{19}$$

Substituting Equation (19) in Equation (5) with the new control signal $\vec{m}_{ctrl}$ the new $\mathbf{B}$ matrix for the state space system is time variant due to the variation of the magnetic field vector as seen from the orbit coordinate system.

$$\mathbf{B}(t) = \begin{bmatrix} \mathbf{I}^{-1} \begin{bmatrix} 0 & -{}^oB_z(t) & {}^oB_y(t) \\ {}^oB_z(t) & 0 & -{}^oB_x(t) \\ -{}^oB_y(t) & {}^oB_x(t) & 0 \end{bmatrix} \\ \begin{bmatrix} 0 & 0 & 0 \\ 0 & 0 & 0 \\ 0 & 0 & 0 \end{bmatrix} \end{bmatrix}. \tag{20}$$

Calculating the rank of the controllability matrix of the state space system for a magnetic field vector of a typical CubeSat orbit and with an inertia matrix for a non perfectly symmetric satellite actually shows that the system has full rank. This implies that the system should be controllable. But when calculating the condition of the controllability matrix the value is greater than 10^{10} which shows that the controllability matrix is nearly singular.
When the extremely small components of the cross coupling through the orbital angular rate are neglected and the satellite is assumed to be perfectly symmetric, the controllability matrix has a reduced rank of 4. This reflects the fact that the rotation and the angular velocity along the magnetic field vector are not controllable.

5.2 Constant Gain Controller

The periodic nature of an idealized linear system will be used to design the constant gain controller. The stability of this controller will be verified using Floquet Theory and evaluation of the results gained from Floquet Theory also allow for an optimization of the controller.

5.3 Periodic Magnetic Field

The controller design described in the following section is based on the assumption of a linear periodic system. Since the orbit for most CubeSats will be circular, the orbital rate ω_0 can be considered to be nearly constant and hence the matrix $\mathbf{A}$ of the state space model as well. In contrast the matrix $\mathbf{B}(t)$ will highly depend on the present magnetic field.

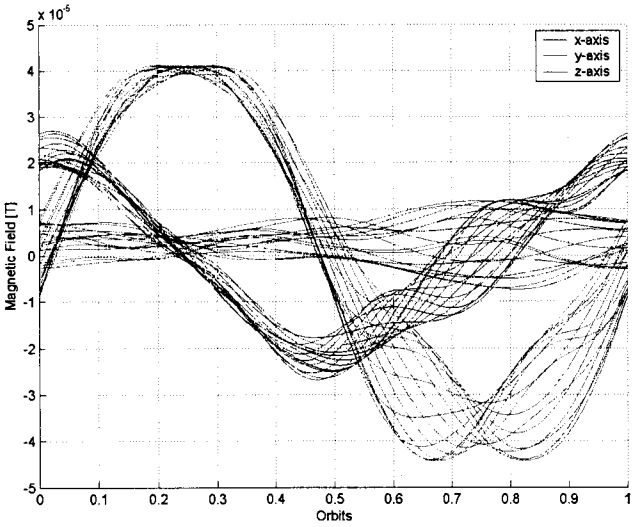

Fig. 2: Magnetic field as seen from the Orbit CS over 15 orbits

Fig. 2 shows the magnetic field as seen from the orbit coordinate system during 15 consecutive orbits. The orbit shown is a typical CubeSat orbit as the one planned orbit for the CASSat satellite (see Table 1). For the actual controller design an idealized periodic model of the Earth's magnetic field is necessary. This is calculated by averaging the magnetic field over 15 orbits (approximately the entire globe is covered after 15 orbits).

$$(21) \qquad {}^{o}\vec{B}(t)_{ave} = \frac{1}{N}\sum_{i=1}^{N} {}^{o}\vec{B}(t)$$

5.4 Mapping Function

The controller can only apply torques that are perpendicular to the magnetic field vector. Thus, an energy optimal control law only generates the magnetic dipole moment that is perpendicular to the magnetic field vector, since parallel components do not influence the generated torque.

$$(22) \qquad {}^{b}\vec{T}_{ctrl} = \left({}^{b}\vec{m}_{\parallel} + {}^{b}\vec{m}_{\perp}\right) \times {}^{b}\vec{B} = {}^{b}\vec{m}_{\perp} \times {}^{b}\vec{B}$$

In [9] the following mapping function is suggested to ensure that the generated magnetic moment by the coils is perpendicular to the magnetic field vector

$$(23) \qquad \vec{u}_{ctrl} \rightarrow {}^{b}\vec{m} \qquad {}^{b}\vec{m} = \frac{\vec{u}_{ctrl} \times {}^{b}\vec{B}}{\| {}^{b}\vec{B} \|}$$

The advantage of this mapping is that the control signal $\vec{u}$ can be chosen arbitrary by the controller. The control torque in the state space system of Equation (5) must now be replaced by

$$(24) \qquad {}^{b}\vec{T}_{ctrl} = \left({}^{b}\vec{u} \times {}^{b}\vec{B}\right) \times {}^{b}\vec{B}$$

which leads to a time variant matrix $\mathbf{B}(t)$.

5.5 Time-invariant System

To apply standard control techniques the equivalent time invariant system has to be found. This is done by substituting the time variant matrix $\mathbf{B}(t)$ with the average value of the matrix over one orbital period T

$$(25) \qquad \mathbf{B} = \frac{1}{T}\int_0^T \mathbf{B}(t)dt$$

This results in the time invariant system

$$(26) \qquad \begin{bmatrix} \delta\dot{\vec{\omega}} \\ \delta\dot{\vec{q}} \end{bmatrix} = \mathbf{A}\begin{bmatrix} \delta\vec{\omega} \\ \delta\vec{q} \end{bmatrix} + \mathbf{B}\vec{u}$$

Calculating the rank and the condition of the controllability matrix shows that the system is controllable, so a linear quadratic regulator design can be used to calculate the constant gain matrix for the feedback. Without loss of generality the weighting matrix $\mathbf{R}$ is set equal to the unity matrix $\mathbf{E}$. The optimal control signal is then found by calculating

$$(27) \qquad \vec{u} = -\mathbf{B}^T\mathbf{P}\begin{bmatrix} \delta\vec{\omega} \\ \delta\vec{q} \end{bmatrix}$$

with $\mathbf{P}$ being the solution of the algebraic Riccati equation

$$(28) \qquad \mathbf{PA} + \mathbf{A}^T\mathbf{P} - \mathbf{PBB}^T\mathbf{P} + \mathbf{Q} = \mathbf{0}.$$

5.6 Time-variant System

The control signal computed in Equation (27) for the time invariant system leads to the following time variant closed loop system when taking the present magnetic field into account

$$(29) \qquad \begin{bmatrix} \delta\dot{\vec{\omega}} \\ \delta\dot{\vec{q}} \end{bmatrix} = \left(\mathbf{A} - \mathbf{B}(t)\mathbf{B}^T\mathbf{P}\right)\begin{bmatrix} \delta\vec{\omega} \\ \delta\vec{q} \end{bmatrix}$$

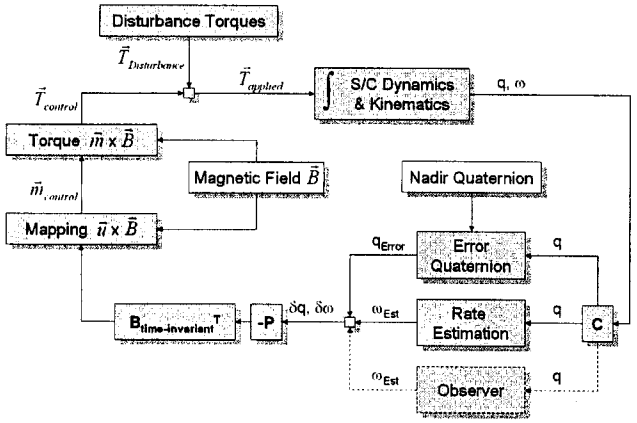

Fig. 3: Flowchart of the Constant Gain Controller Design for the time variant system

The flowchart of the satellite system and the controller can be seen in Fig. 3.
However a controller that guarantees stability for the time invariant linear system guarantees stability neither for the linearized time variant satellite model nor for the actual nonlinear model and thus the stability has to be further examined.

5.7 Stability of the Controller

The linear system used to solve the algebraic Riccati Equation (28) contains some simplifications so the solution does not guarantee stability for the actual non linear satellite model.
However the stability of the time-variant counterpart of the time-invariant system can be examined and verified using Floquet Theory described in [10] and [8] since with the periodic magnetic field calculated previously the system can be considered as a periodic linear time-variant system.
For the examination using Floquet Theory Equation (29) is now rewritten as

$$\dot{\vec{x}} = \mathbf{A}(t)\vec{x} \tag{30}$$

with

$$\vec{x} = \begin{bmatrix} \delta\vec{\omega} \\ \delta\vec{q} \end{bmatrix}, \qquad \mathbf{A}(t) = \left(\mathbf{A} - \mathbf{B}(t)\mathbf{B}^T\mathbf{P}\right) \tag{31}$$

and

$$\mathbf{A}(t) = \mathbf{A}(t+T), \text{ due to } \mathbf{B(t)} = \mathbf{B}(t+T). \tag{32}$$

The system has the following solution

$$x(t) = \phi(t, t_0)x(t_0) \tag{33}$$

with ϕ being the state transition matrix of the system. The Equations (30) and (33) lead to an equation for $\dot{\phi}$

$$\dot{x} = \mathbf{A}(t)x(t) = \mathbf{A}(t)\phi(t, t_0)x(t_0) \tag{34}$$

$$\dot{\phi}(t, t_0)x(t_0) = \mathbf{A}(t)\phi(t, t_0)x(t_0) \tag{35}$$

Since Equation (35) shall be valid for arbitrary values of $x(t_0)$ the equation for $\dot{\phi}$ can be concluded

$$\dot{\phi}(t, t_0) = \mathbf{A}(t)\phi(t, t_0), \qquad \phi(t_0, t_0) = \mathbf{E}. \tag{36}$$

The state-transition-matrix is very important for the use of the Floquet Theory. Taking Equation (36) into account the following identity can be shown

$$\phi(t + T, t_0) = \phi(t, t_0)\mathbf{C}. \tag{37}$$

Then there exists a constant matrix $\mathbf{R}(T)$ such that

$$\mathbf{C} \equiv e^{\mathbf{R}(T)} \tag{38}$$

It now can be shown that

$$\phi(t, t_0) = \mathbf{P}(t, t_0)e^{\mathbf{R}(t-t_0)}, \tag{39}$$

with $\mathbf{P}$ being a periodic matrix

$$\mathbf{P}(t + T, t_0) = \mathbf{P}(t, t_0) \tag{40}$$

From Equation (39), with $\phi(t_0, t_0) = \mathbf{P}(t_0, t_0) = e^{\mathbf{R}(t_0-t_0)} = \mathbf{I}$, it is seen at $t = t_0 + T$ that

$$\phi(t + T, t_0) = \mathbf{P}(t_0 + T, t_0)e^{\mathbf{R}T} = e^{\mathbf{R}T}. \tag{41}$$

The matrix $\phi(t+T, t_0)$ is called the monodromy matrix $\psi(t_0)$. With $x(t) = \phi(t, t_0)x(t_0)$ being the solution for $\dot{x} = \mathbf{A}x$, it can be seen from Equation (41) that the solution consists of a periodically modulated exponential matrix function. Therefore the system is asymptotically stable if the eigenvalues of $\mathbf{R}$ all have negative real parts. The demand that

$$\begin{aligned} det[\mathbf{I}\varphi - \mathbf{R}] &= 0 \\ Re(\varphi_i) &< 0 \end{aligned} \tag{42}$$

is equivalent to

$$\begin{aligned} det[\mathbf{I}\lambda - \boldsymbol{\psi}] &= 0 \\ |\lambda_i| &< 1 \end{aligned} \tag{43}$$

So a linear periodic system is asymptotically stable if the eigenvalues of the monodromy matrix, which is the state transition matrix after one period, are on the open unit disk. The smaller the absolute values of the monodromy matrix are, the faster and more robust the controller is. Therefore the eigenvalues should be as close to zero as possible.
With this background the steps to verify the stability of a linear periodic system are:

Step 1:
Calculate the monodromy matrix $\psi(t_0) = \phi(t_0+T, t_0)$ by numerical integration of

$$\dot{\phi}(t, t_0) = \mathbf{A}(t)\phi(t, t_0). \tag{44}$$

$$\psi(t_0) = \int_0^T \mathbf{A}(t)\phi(t, t_0). \tag{45}$$

with the initial condition $\phi(t_0, t_0) = \mathbf{E}$.

Step 2:
Evaluate the absolute value of the eigenvalues of the monodromy matrix ψ.

Step 3:
Check the stability conditions $|\lambda_i| < 1$

5.8 Optimization

Hand in hand with checking the stability condition by securing that the eigenvalues of the monodromy matrix are smaller than one goes the optimization of the controller. As it can be concluded from Equation (41) the damping and the speed of the controller are increased with minimizing the maximum absolute value of the eigenvalues of the monodromy matrix. Thus, the cost function $f(x)$ that has to be minimized is defined as

$$f(x) = max\,|eig\,(\psi(t_0))|\,. \tag{46}$$

The entries of the feedback matrix $\mathbf{P}_{opti}$ are varied with $\psi(t_0)$ calculated using

$$\psi(t_0) = \int_0^T \mathbf{A}_{opti}(t)\phi(t, t_0)$$

with

$$\mathbf{A}_{opti}(t) = \left(\mathbf{A} - \mathbf{B}(t)\mathbf{B}^T\mathbf{P}_{opti}\right).$$

The optimization algorithm uses the negative gradient of the cost function as the search direction. Nested intervals are used to find the minimum during the one-dimensional minimum search. The optimization is unconstrained.

6 SIMULATIONS

The CASSat simulation results presented in the following are based on the orbital parameters given in Table 1. As afore mentioned the constant gain controller is highly dependant on the orbit and the feedback matrix in this example has been calculated and optimized for this orbit. The desired attitude in the simulation example is the nadir pointing mode. With an inclination of about 98 degrees this orbit is a polar orbit. This implies that the component of the magnetic field vector perpendicular to the orbital plane is almost zero as it can also be seen in Fig. 2. This fact further complicates the attitude control.

Parameter		Value	
Semi major axis	a =	7202.9	[km]
Eccentricity	e =	0.0023	
Inclination	i =	98.7243	[Deg]
RAAN	Ω =	-93.9955	[Deg]
Argument of Perigee	ω =	94.6541	[Deg]
Initial true anomaly	θ =	295.3831	[Deg]

Table 1: *Initial orbital parameters for the simulation of the attitude controller*

The model for the magnetic field is essential for the design of the attitude controller. For the controller design and for the simulation model the International Geomagnetic Reference Field (IGRF) model [11] was selected. The coefficients for this magnetic field model are updated every five years. The latest coefficients available were issued for the year 2005, but since this research was started in 2004, the coefficients valid for 2000 are implemented. Coefficients for the linear extrapolation of the magnetic field model for the years between the releases of the field coefficients are provided as well.

6.1 Environment

To provide realistic data about the detumbling time of the satellite and the attitude pointing accuracy achievable disturbance torques have to be considered. The following torques were identified as main disturbances:

- Aerodynamic Torque
- Radiation Torque
- Gravity Gradient Torque
- Residual Magnetic Dipole

The density of the upper atmosphere plays an important roll in the calculation of the aerodynamic torque. Several models with an increasing complexity are available. No own implementation was created, but an already existing Harris-Priest Density Model implementation was used [12].

The aerodynamic torque and the radiation torque depend on the deviation of the centre of pressure to the centre of mass (CoM). Within the CubeSat standard a maximum deviation of 20 mm from the centre of mass to the geometric centre is allowed. This maximum deviation was considered as lever-arm of the acting forces.
The gravity gradient torque can be a disturbance torque or it can be used for passive stabilization when flying in a nadir pointing flight mode. Since the controller design should be examined without other means but magnetorquers the mass properties were chosen is such a way that no gravity gradient occurred or in a way that the resulting torque acted as a disturbance torque.
The residual magnetic dipole was not considered as a disturbance torques because it is the only torque that can be fully compensated by the magnetorquers and can just be added into the control law as a bias.

6.2 Detumbling-Controller

The simulation of the detumbling controller introduced shows that detumbling is possible within less than half an orbital period as it can be seen in Fig. 4. It was assumed that the satellite has an angular velocity of 0.1 rad/s after the deployment.

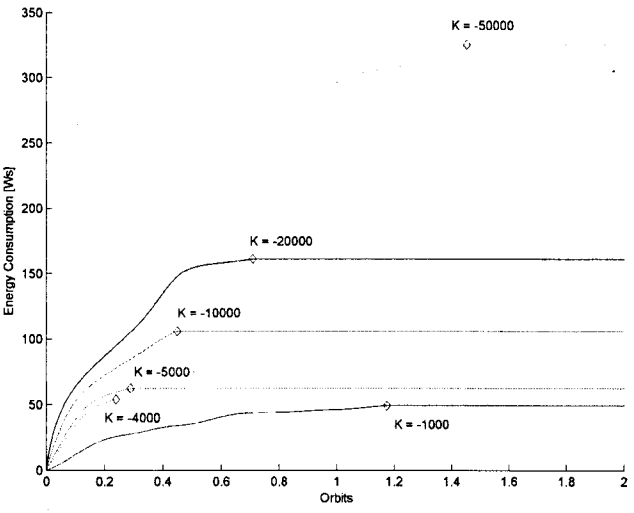

Fig. 4: Energy consumption and time demand of the detumbling process for different values for the feedback matrix $K_{control}$

The detumbling process shows no obvious dependency on the presence of disturbance torques. Within the simulations the time to detumble the satellite to the required rate of 0.03 rad/s varied barely and was sometimes decreased by the disturbance torques. The discretization of the controller also showed little influence on the behavior during the simulations.
An interesting effect could be observed during the optimization of the detumbling process. The feedback matrix $K_{control}$ was varied and one would expect the detumbling process to be faster when increasing the values of $K_{control}$ since the torques to detumble the satellite are higher. This is true for two axes of the satellite whose angular velocities are reduced with increasing speed due to a higher value in $K_{control}$.

However, the third axis then gets aligned with the magnetic field vector and thus no torques can be applied to the remaining axis. For the highest value of $K_{control}$ simulated "steps" in the angular velocity of the remaining axis can be observed in Fig. 5. These steps occur when the satellite passes the poles and the magnetic field vector changes its direction rapidly and thus a better detumbling of the remaining axis is possible.

Another effect that can be observed in Fig. 4 is the increasing energy consumption for higher feedback values in $K_{control}$. This is due to the fact that the control torques to reduce the angular velocity on the remaining axis are not applied in an optimal way and thus more energy is consumed.

Thus, to detumble all three axis in an optimal way the $K_{control}$ matrix must be sufficiently low.

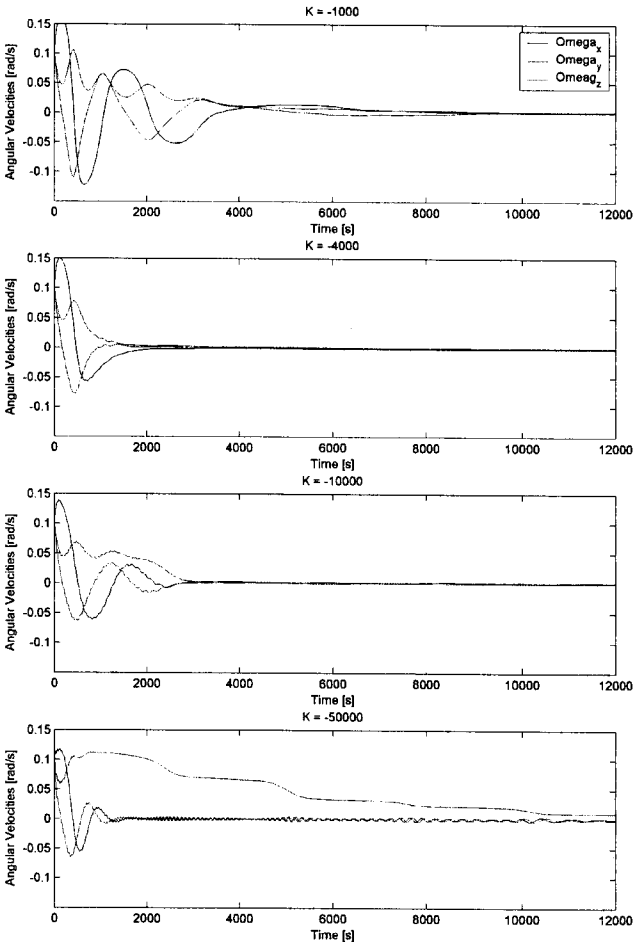

Fig. 5: Detumbling of the satellite with different values for the feedback matrix $K_{control}$

6.3 3-Axis-Controller

The simulations of the implemented 3-axes controller show that it is theoretically possible to stabilize the satellite by only using magnetorquer as it is shown in the plot at the top of Fig. 6. The time to attain the desired attitude from an arbitrary initial condition is about four orbits.
Assuming the maximum disturbance torques that can occur within the specifications of the CubeSat standard a 3-axes attitude control with a reasonable pointing accuracy can not be achieved. In a worst case scenario deviations of more than 90 degrees can occur as shown in the middle of Fig. 6. This results from the fact that disturbance torques parallel to the magnetic field can not be compensated and accumulate.

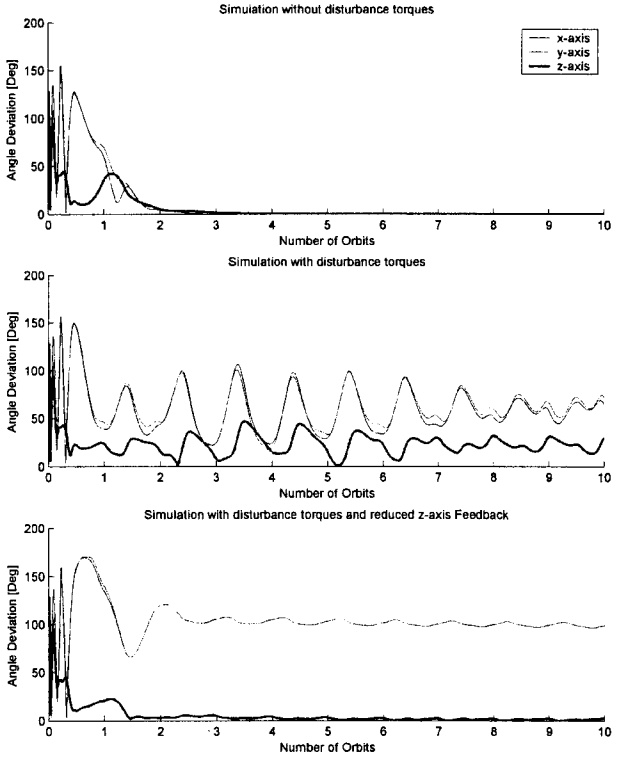

Fig. 6: *Angle deviation of desired acquisition axis for simulations without and with disturbance torques and with disturbance torques and reduced feedback on the z-axis (sensor axis)*

However, if the satellite is build in such a way that the disturbance torques are minimized a pointing accuracy of better than 5 degrees can be achieved. Thus, during the further satellite design any action should be taken to avoid disturbance torques on the satellite. Additionally when flying in nadir pointing mode the gravity gradient can be used to provide a supplemental passive stabilization.
If the avoidance of disturbance torques is not possible and the satellite will experience disturbance torques greater than the ones acceptable for the pointing accuracy, the controller design can still be optimized manually for pointing the sensor-axis with the necessary accuracy.
However, the price to pay for the accuracy on the sensor axis is the loss of accuracy on the remaining axes. To avoid internal "disturbance torques" on the sensor-axis due to non optimal application of control torques for adjusting the remaining axes the entry of the feedback matrix $\mathbf{P}$ for the control of the rotation about the sensor-axis can be decreased manually.
The satellite will then be rotated to an attitude were the sensor-axis is aligned with the nadir direction at its best and the disturbance torques about the sensor-axis are minimized. The rotation about the sensor-axis can be seen as some kind of passive stabilization in an arbitrary direction. The disturbance torques about the sensor-axis will rotate the satellite in such a position so that there is an equilibrium as shown in the bottom plot of Fig. 6.
The minimization of the disturbance torques due to the rotation about the sensor-axis can be observed in Fig. 7.

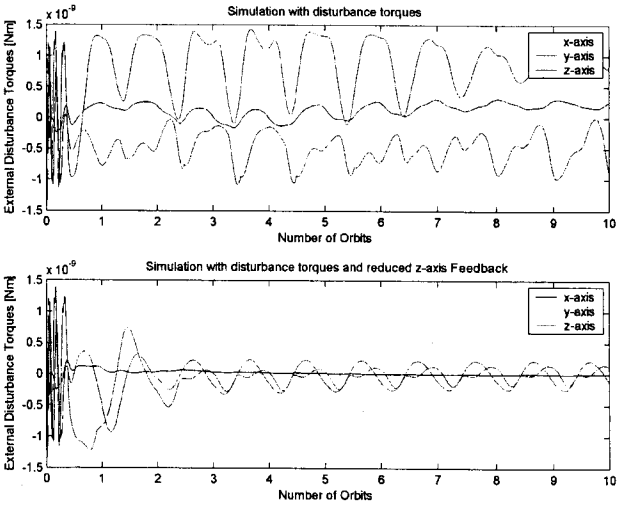

Fig. 7: *Disturbance torques acting on the satellite with full feedback and disturbance torques acting on the satellite with reduced feedback on the z-axis (sensor-axis). The disturbance torques rotate the satellite in such a way that the lever arm of the disturbance force is minimized*

Discretization of the controller barely affected the stabilization of the satellite. Simulations with the discretized controller showed almost the same behavior as the continuous one.

7 SUMMARY

To tackle the problem of attitude control on a micro satellite conforming with the CubeSat standard and with no other active or passive attitude control but magnetorquers, the possible controllers to be implemented were reviewed. Due to the limitations on a

CubeSat a constant gain controller was chosen for the 3-axes control of the satellite. The detumbling after ejection from the P- or T-Pod is performed by a very robust B-dot controller that only relies on the measurements of the magnetometer.
The stability of the B-dot controller was verified using Lyapunov Theory and the optimization of the feedback matrix was performed manually. The values of the feedback matrix may not be chosen too high since otherwise the detumbling process will become time and energy consuming due to the alignment of a principal axis with the magnetic field vector.
To design the constant gain controller a linearization of the equations of motion was performed about the desired setpoint and by generating a periodic magnetic field model a linear periodic system was derived. The stability and optimization of the 3-axis controller was accomplished using Floquet Theory.
The simulations with the IGRF magnetic field model showed that the detumbling of the satellite can be performed within less than half an orbit and that the detumbling process is little influenced by perturbation torques.
Simulations with the optimized 3-axis controller revealed that without reducing the disturbance torques on the satellite by constructional means a reasonable pointing accuracy can not be achieved. If these constructional measures can not be implemented a magnetic actuation system is still able to achieve the desired pointing accuracy on one axis.

References

[1] Søren Vijlgaard Vedstesen Torben Graversen, Michael Kvist Frederiksen. *Attitude Control System For AAU CubeSat.* Master thesis, Aalborg University, 2002.

[2] Wiley J. Larson James Wertz. *Space Mission Analysis and Design.* Kluwer Academic, Dordrecht, London, 1999.

[3] James Wertz. *Spacecraft Attitude Determination and Control.* D. Reidel Publishing Company, Dordrecht, Netherlands, 1978.

[4] Vladimir A. Chobotow. *Spacecraft Attitude Dynamics and Control.* Krieger Publishing Company, Malabar, Florida, 1991.

[5] Florian Renk. *Attitude Control for a Micro Satellite using only Magnetic Coils and Target Pointing for Multiple Satellites.* Thesis, Institut für Flugmechanik und Flugregelung, Universität Stuttgart, Australian Centre for Field Robotics, The University of Sydney, 2004.

[6] Attilio Salvetti Angelo Miele. *Applied Mathematics in Aerospace Science and Engineering.* Plenum Press, New York, 1994.

[7] Tanja Staebler. *Nichtlinear Regelung und neuronale Netze.* Lecture notes, The University of Stuttgart, Institut für Flugmechanik und Flugregelung, 2001.

[8] Walter Fichter. *Advanced Spacecraft Navigation and Control.* Lecture notes, The University of Stuttgart, 2004.

[9] Rafal Wiesniewski. *Satellite Attitude Control Using Only Electromagnetic Actuation.* Phd, Aalborg University, 1996.

[10] Ronald R. Mohler. *Nonlinear Systems, Dynamics and Control, Volume 1.* Prentice-Hall, Inc., Englewood Cliffs, New Jersey, 1991.

[11] The International Association of Geomagnetism and Aeronomy. *Geomagnetic Models and Software.* National Geophysical Data Center (NGDC), http://www.ngdc.noaa.gov/seg/geomag/geomag.shtml, 2005.

[12] W. Priest I. Harris. *Time-Dependent Structure of the Upper Atmosphere.* NASA TN D-1443, Goddard Space Flight Center, Maryland, 1962.